Macrolide antibiotics activate the integrated stress response and promote tumor proliferation

Xin Yu[1,#], Ai-Ling Tian[2,3,4,5,#], Ping Wang[6,#], Juanjuan Li[1], Juan Wu[7], Bei Li[7], Zhou Liu[1], Siqing Liu[1], Zhijie Gao[1], Si Sun[8], Shengrong Sun[1,*], Yi Tu[1,*] and Qi Wu[9,*]

[1] Department of Breast and Thyroid Surgery, Renmin Hospital of Wuhan University, Wuhan, Hubei, P. R. China.
[2] Gustave Roussy Cancer Campus, Villejuif Cedex, France.
[3] Université Paris-Saclay, Faculté de Médecine, Le Kremlin-Bicêtre, France.
[4] Centre de Recherche des Cordeliers, INSERM U1138, Équipe Labellisée - Ligue Nationale contre le Cancer, Université Paris Cité, Sorbonne Université, Paris, France.
[5] Metabolomics and Cell Biology Platforms, Gustave Roussy Cancer Campus, Villejuif, France.
[6] Medical College, Anhui University of Science and Technology, Huainan, AnHui, P. R. China.
[7] Department of Pathology, Renmin Hospital of Wuhan University, Wuhan, Hubei, P. R. China.
[8] Department of Clinical Laboratory, Renmin Hospital of Wuhan University, Wuhan, Hubei, P. R. China.
[9] Tongji University Cancer Center, Shanghai Tenth People's Hospital, School of Medicine, Tongji University, Shanghai, P. R. China.
[#] These authors have contributed equally to this work and share first authorship.
[*] Corresponding Authors:
Dr. Qi Wu, Tongji University Cancer Center, Shanghai Tenth People's Hospital, School of Medicine, Tongji University, Shanghai, P. R. China; E-mail: waiwai@whu.edu.cn
Dr. Yi Tu, Department of Breast and Thyroid Surgery, Renmin Hospital of Wuhan University, 238 Ziyang Road, Wuhan 430060, Hubei Province, P. R. China; E-mail: rm000750@whu.edu.cn
Dr. Shengrong Sun, Department of Breast and Thyroid Surgery, Renmin Hospital of Wuhan University, 238 Ziyang Road, Wuhan 430060, Hubei Province, P. R. China; E-mail: sun137@sina.com

IN PRESS

ABSTRACT Macrolide antibiotics are widely used antibacterial agents that are associated with autophagy inhibition. This study aimed to investigate the association between macrolide antibiotics and malignant tumors, as well as the effect on autophagy, reactive oxygen species (ROS) accumulation and integrated stress response (ISR). The meta-analysis indicated a modestly higher risk of cancer in macrolide antibiotic ever-users compared to non-users. Further experiments showed that macrolides block autophagic flux by inhibiting lysosomal acidification. Additionally, azithromycin, a representative macrolide antibiotic, induced the accumulation of ROS, and stimulated the ISR and the activation of transcription factor EB (TFEB) and TFE3 in a ROS-dependent manner. Finally, animal experiments confirmed that azithromycin promoted tumor progression *in vivo*, which could be receded by N-acetylcysteine, an inhibitor of ROS and ISR. Overall, this study reveals the potential role of macrolide antibiotics in malignant progression and highlights the need for further investigation into their effects.

INTRODUCTION

As one of the most extensively applicable agents, the use of antibiotics has emerged to bring questionable advances in the therapeutic strategies of patients with cancer. In-creasing evidence indicates that long-term or inappropriate antibiotic abuse is linked to an increased risk of cancer [1-4]. In addition, the overuse of antibiotic therapy is attributable to resistance to chemotherapy and immunotherapy

[5-7]. However, targeted antimicrobial therapy can reduce the incidence and mortality of gastric cancer caused by *Helicobacter pylori*, which is a well-known risk factor in stomach cancer [8]. Therefore, the rational use of antibiotics in patients with cancer needs further exploration.

Macrolides are compounds that are composed of macrocyclic lactone rings, and are extensively used as antibiotics and immune inhibitors. As a category of antibiotics, they strictly consist of 14-, 15-, or 16-membered lactone rings [9, 10]. For example, erythromycin and roxithromycin (RA) possess the structure of 14-lactone rings, azithromycin (AZD) belongs to the family of 15-lactone rings, and the representative agent consisting of 16-lactone rings is spiramycin (SP) [9]. Additionally, tacrolimus and sirolimus possessing of macrolide amide structures have been used as immunosuppressants or immunomodulators after liver or renal transplantation and for treatment of autoimmune disease [11, 12]. In clinical practice, macrolide antibiotics are first-line drugs for typical community-acquired pneumonia and chlamydia infection. Moreover, macrolide antibiotics, including brefeldin A and AZD, exert considerable antitumour effects both *in vitro* and *in vivo* [13-15]. Likewise, macrolide antibiotics could restore the sensitivity of tumor cells to agents, bortezomib, CDK4/6 inhibitors, or EGFR-TKIs [16-19]. However, there is evidence suggesting that the prophylactic use of AZD can increase the incidence of haematological relaxation by 70% two years after haematopoietic cell transplantation [20]. Besides, exposure to AZD is associated with an increased risk of subsequent neoplasm after hematopoietic cell transplantation [21]. Therefore, the potential role of macrolide antibiotics in malignant progression requires further exploration.

The integrated stress response (ISR) is characterized by the phosphorylation of the eukaryotic initiation factor 2α (eIF2α) [22]. As a phylogenetically conserved protein, eIF2α can be phosphorylated by four main kinases: heme-regulated inhibitors, general control nonderepressible-2, protein kinase double-stranded RNA-dependent (PKR) and PKR-like endoplasmic reticulum (ER) kinase (PERK) [23]. ISR has a pivotal effect on the adaptation to oxidative stress or ER stress, initiation of autophagy, mitochondrial homeostasis, and innate cellular defense against viral infections [22, 24-26]. However, ISR has been shown to promote the growth and metastasis of malignant tumors by inducing epithelial-mesenchymal transition (EMT) and angiogenesis [27]. Moreover, the crucial lysosomal transcription factors, transcription factor EB (TFEB) and TFE3, have been found to mediate the cellular response to ISR [28]. PERK and phosphorylated eIF2α activate TFEB and TFE3 after treatment with lysosomotropic agents (such as AZD) and ER stressors (such as thapsigargin (TG) and tunicamycin (TM)) [28, 29]. Macrolides such as AZD are known to be trapped in lysosomes by enhancing protonation under acidic conditions, leading to lysosomal acidification dysfunction and lysosomal function blockage via increases in their concentration in the lysosome until lysosomal membranes are destabilized [30, 31]. Our previous results indicate that lysosomotropic agents including 3-hydroxychloroquine, chloroquine, and AZD, have the capacity to stimulate ISR by blocking autophagic flux, resulting in the activation of TFEB and TFE3 [29]. Potentially, macrolide antibiotics may affect malignant biological properties by inducing ISR.

In this work, macrolide antibiotics were identified as potent autophagy inhibitors that induce a loss of lysosomal acidification. Furthermore, the representative agent, AZD, induced the accumulation of intracellular reactive oxygen species (ROS) and stimulated ISR, leading to the activation of TFEB and TFE3. Ultimately, treatment with AZD accelerated tumor growth.

RESULTS

Meta-analysis indicated a correlation between the use of macrolide antibiotics and an increased risk of malignant tumors

Previous studies have suggested that the overuse of antibiotics can increase the risk of cancer and reduce the efficacy of chemotherapy and immunotherapy [1-3, 5-7]. To further investigate the association of macrolide antibiotic use with tumors, we retrospectively searched and identified 36,578 publications. Ten studies, including 825,068
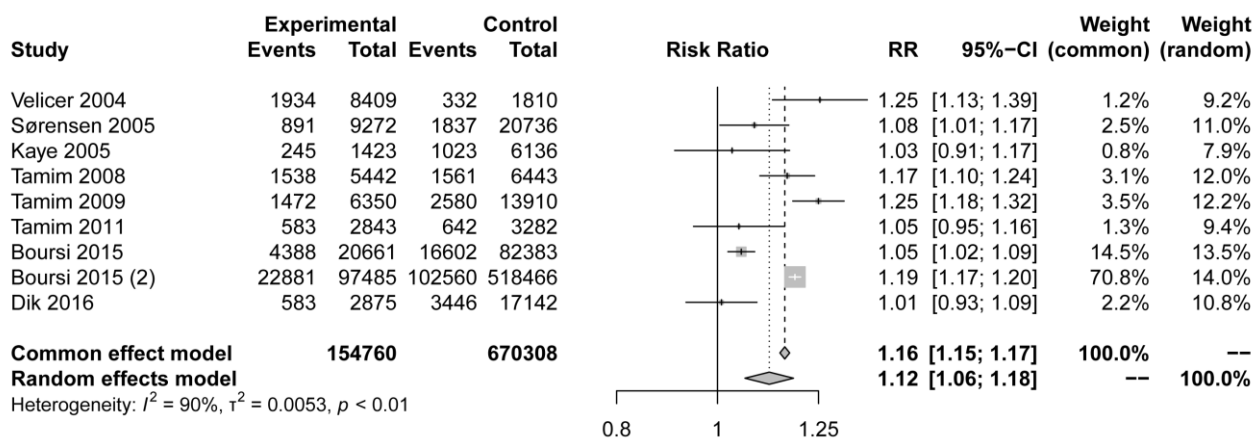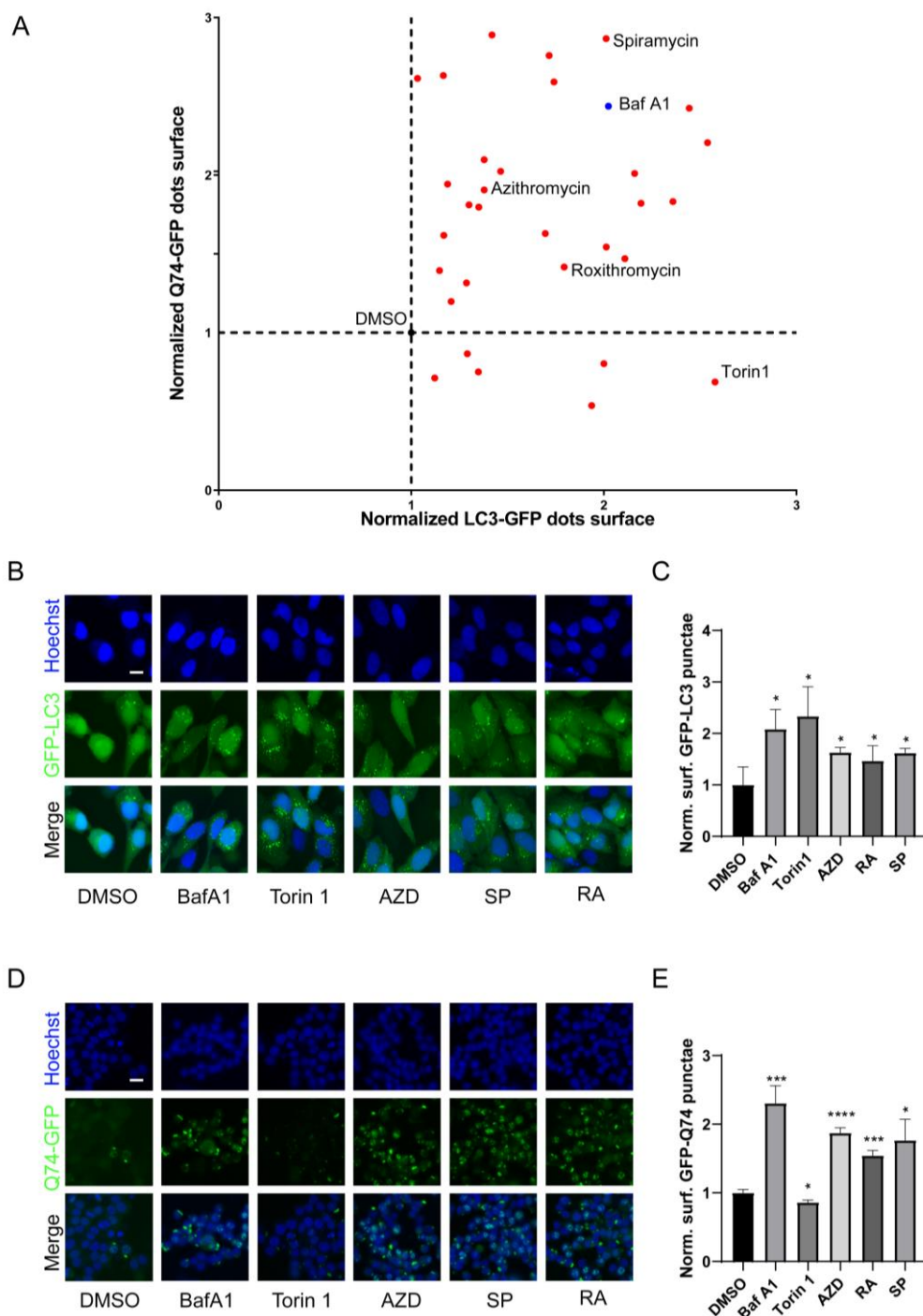

Study	Experimental Events	Total	Control Events	Total	Risk Ratio	RR	95%−CI	Weight (common)	Weight (random)
Velicer 2004	1934	8409	332	1810		1.25	[1.13; 1.39]	1.2%	9.2%
Sørensen 2005	891	9272	1837	20736		1.08	[1.01; 1.17]	2.5%	11.0%
Kaye 2005	245	1423	1023	6136		1.03	[0.91; 1.17]	0.8%	7.9%
Tamim 2008	1538	5442	1561	6443		1.17	[1.10; 1.24]	3.1%	12.0%
Tamim 2009	1472	6350	2580	13910		1.25	[1.18; 1.32]	3.5%	12.2%
Tamim 2011	583	2843	642	3282		1.05	[0.95; 1.16]	1.3%	9.4%
Boursi 2015	4388	20661	16602	82383		1.05	[1.02; 1.09]	14.5%	13.5%
Boursi 2015 (2)	22881	97485	102560	518466		1.19	[1.17; 1.20]	70.8%	14.0%
Dik 2016	583	2875	3446	17142		1.01	[0.93; 1.09]	2.2%	10.8%
Common effect model		**154760**		**670308**		**1.16**	**[1.15; 1.17]**	**100.0%**	**−−**
Random effects model						**1.12**	**[1.06; 1.18]**	**−−**	**100.0%**

Heterogeneity: $I^2 = 90\%$, $\tau^2 = 0.0053$, $p < 0.01$

FIGURE 1: Forest plot examining the association between macrolide antibiotic ever-use versus nonuse and the risk of cancer.
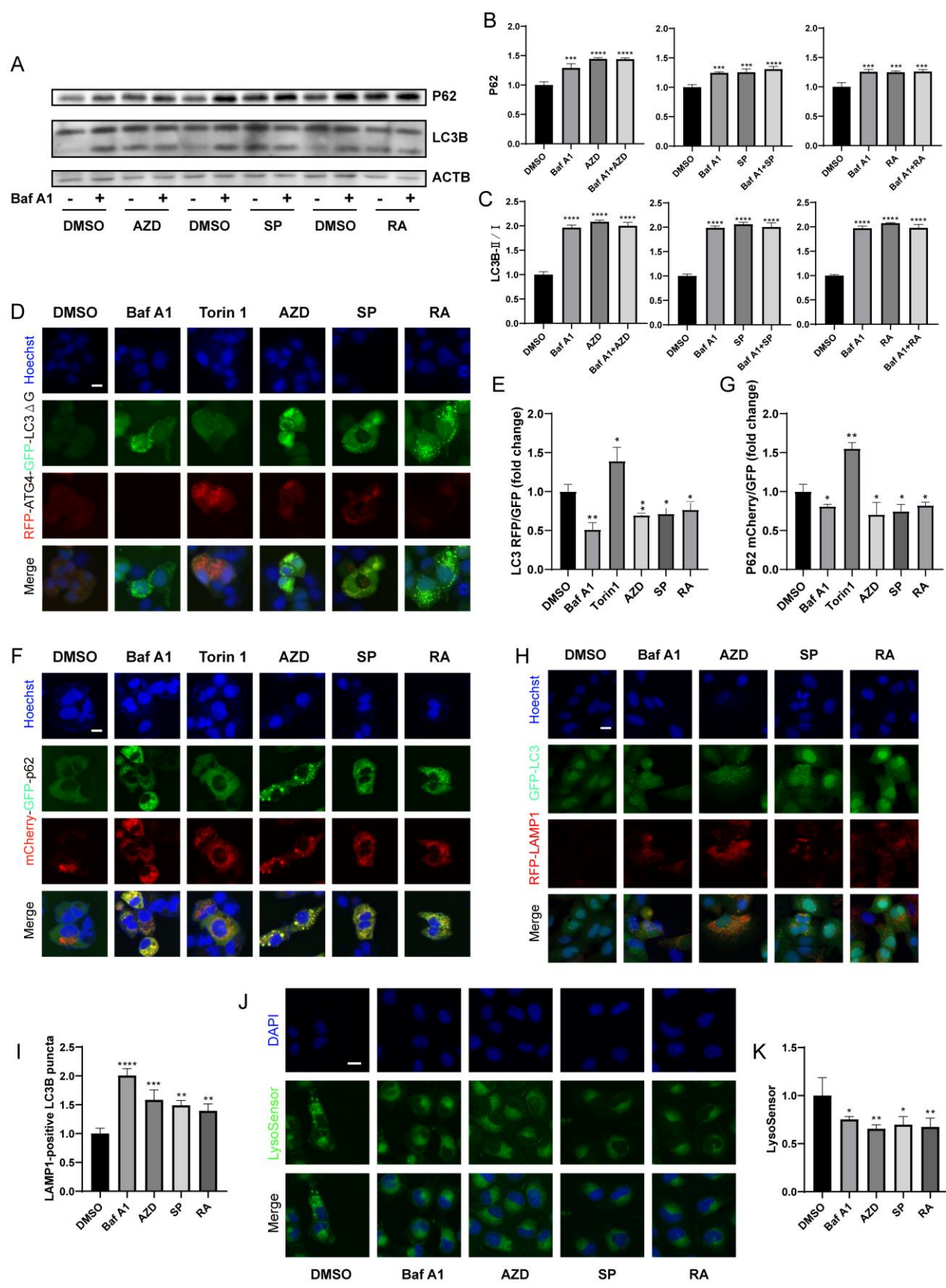
individuals and over 154,760 malignant tumor cases, met the eligibility criteria (Fig. S1, Table S1) [32-41]. The studies included were published in English from 2008 to 2015. Three studies were conducted in Canada [35, 37, 38], three in the UK [34, 39, 40], one in the USA [32], one in Denmark [33] and one in the Netherlands [41]. Studies included various cancer types, such as breast, lung, and colorectal cancer, etc.

The pooled risk estimate indicated that compared to non-users, macrolide antibiotic ever-users had a modestly

higher risk of cancer (RR=1.12,95% CI 1.06-1.18, **Fig. 1**). Although the meta-analysis showed statistical heterogeneity among the studies (I^2 = 90%), no evidence indicated a significant influence in any single study (Fig. S1A). Asymmetrical towards positive associations was not presented in the funnel plot (Fig. S1B), revealing no significant publication bias (Egger's test p=0.2467). In conclusion, our meta-analysis showed that the use of macrolide antibiotics was associated with a higher incidence of malignancy, but the mechanism requires further exploration.

FIGURE 2: Identification of macrolide antibiotic as potent blockers of autophagic flux. (A) GFP-LC3B-expression U2OS cells and GFP-Q74-expression PC12 cells were treated with Torin 1 (300 nM), Baf A1 (100 nM) or macrolides (40 µM) for 6 h. **(B, C)** GFP-LC3-expression U2OS cells or **(D, E)** GFP-Q74-expression PC12 cells were treated with torin 1, Baf A1, AZD (40 µM), RA (40 µM) or SP (40 µM) for 6 h. Representative images are presented **(B, D)**. The **(C)** GFP-LC3B or **(E)** GFP-Q74 puncta were assessed. Scale bars equal 10 µm. *P<0.05; **P < 0.01; ***P < 0.001; **** P < 0.0001 compared with DMSO/control.

FIGURE 3: Macrolide antibiotics block the autophagy flux. (A) U2OS cells were treated with AZD (40 μM), RA (40 μM) or SP (40 μM) combined or not with Baf A1 (10 nM) for 4 h. Then the western blot was conducted. And the relative expression of P62 and LC3B Ⅱ / Ⅰ was calculated **(B, C)**. **(D, E)** GFP-ATG4-RFP-LC3BΔG-expression and **(F, G)** mCherry-GFP-p62-expression U2OS cells were treated with Torin 1 (300 nM), Baf A1, AZD, RA or SP for 6 h. The fluorescence of GFP and RFP was measured, and the RFP/GFP ratio was calculated **(E, G)**. **(H, I)** GFP-LC3 and RFP-LAMP1 U2OS cells were treated with Baf A1, AZD, RA and SP for 6 h. And the LAMP1-positive LC3B puncta were measured **(I)**. **(J, K)** U2OS cells were treated with Baf A1, AZD, RA and SP for 6 h, and incubated with LysoSensor for 30 min at 37℃. Then the average intensity of lysoSensor fluorescence was assessed **(K)**. Representative images are presented **(J)**. Scale bars equal 10 μm. *P<0.05; **P < 0.01; ***P < 0.001; **** P < 0.0001 compared with DMSO.

Macrolide antibiotics are potential autophagic inhibitors

Macrolides exert their antibacterial effects by interfering with ribosomal function [9], and recent evidence indicates that they can also cause lysosomal acidification disorders [30], which affect the autophagy process. To investigate the influence of macrolides on autophagy, a library of macrolides was screened for their role in autophagic flux through GFP-microtubule-associated proteins 1A/1B light chain 3B (MAP1LC3/LC3B)-expressing U2OS cells and GFP-Q74-expressing PC12 cells (macroautophagy can be detected by measuring the degradation of GFP that aggregates in the cytoplasm) [42]. Similar to Bafilomycin A1 (Baf A1, lysosomal acidification inhibitor), almost all macrolide antibiotics (except kitasamycin) increased puncta of GFP-LC3B and GFP-Q74, while macrolide immunosuppressants increased GFP-LC3B punta but decreased GFP-Q74 puncta, similar to Torin 1 (mechanistic target of rapamycin inhibitor; **Fig. 2A**, Table S2). The stimulating effects of RA, AZD, and SP on GFP-LC3B and GFP-Q74 dots were verified (**Fig. 2B-E**). In summary, macrolide antibiotics induce the accumulation of LC3B and Q74, and appear to be potential inhibitors of autophagy.

Macrolide antibiotics block autophagic flux

Next, we further determined whether macrolide antibiotics block actual autophagic flux. Immunoblot analyses showed that AZD, RA and SP induced the accumulation of P62 and LC3B (**Fig. 3A-C**), and in combination with Baf A1 increased the accumulation of P62 but not LC3B compared to Baf A1 alone, indicating that macrolides block autophagic flux [43]. Besides, RFP-ATG4-GFP-LC3BΔG-expressing U2OS cells were used. Experiments confirmed that AZD, RA and SP consistently decreased the RFP/GFP ratio of cells, indicating a decrease in autophagic flux (**Fig. 3D, E**) [42]. Similarly, mCherry (pH-resistant)/GFP (pH-sensitive) was reduced in mCherry-GFP-sequestosome 1 (SQSTM1/p62) expressing cells treated with AZD, RA and SP (**Fig. 3F, G**). In addition, AZD, RA and SP induced an increase in LAMP1-positive LC3B puncta (**Fig. 3H-I**), but decreased lysosomal acidity assessed by Lysosensor (**Fig. 3J-K**). These results indicate that macrolide antibiotics block autophagic flux by inhibiting lysosomal acidification without hindering autophagosome-lysosome fusion.

AZD induces ROS accumulation and endoplasmic reticulum (ER) stress

When autophagic flux is blocked, misfolded and unfolded proteins accumulate, leading to the unfolded protein response (UPR). In addition, recent studies have shown that

macrolide antibiotics, particularly AZD, inhibit mitochondrial function and increase ROS levels [44], which are known inducers of ER stress and autophagy [45, 46]. Therefore, we used AZD as a representative macrolide antibiotic to investigate the role of macrolide antibiotics in ROS and ER stress. Flow cytometry analysis results showed that AZD induced ROS accumulation in MCA 205 cells, which could be reversed by N-acetylcysteine (NAC), a scavenge of ROS (**Fig. 4A-B**) [45]. Furthermore, AZD induced signs of ER stress like TG and TM (ER stress inducing agents; **Fig. 4C–K**, Fig. S2A-E), including upregulation of phosphorylation of eIF2α on serine 51 (PeIF2α) and GFP-C/EBP homologous protein (CHOP) in U2OS cells (**Fig. 4C-E**, Fig. S2A, B). Other markers of ER stress, including the nuclear presence of activating transcription factor 4 (ATF4) (**Fig. 4F, G**, Fig. S2A, C), ATF6 (**Fig. 4H, I**, Fig. S2A, D), and the spliced isoform of X-box binding protein 1 (XBP1s; **Fig. 4J, K**, Fig. S3 A, E) were also induced by AZD. In addition, ER stress induced by AZD could be reversed by NAC (**Fig. 4C–K**, Fig. S2A-E). These results indicate that AZD is a potent ER stressor that induces the phosphorylation of eIF2α and that this induction is at least partially dependent on accumulation of ROS. Additionally, the accumulation of LC3B and P62 induced by AZD was partially suppressed by NAC (Fig. S2F), while the increase in mRNA levels of LC3B and P62 was significantly inhibited (Fig. S2G, H), suggesting that AZD may promote the intracellular accumulation of LC3B and P62 through two pathways, autophagy blockade and induction of cellular stress.

AZD induces TFEB/TFE3 activation

TFEB and TFE3 are transcription factors that act as master genes controlling lysosomal biosynthesis and autophagy. Their activation is triggered by lysosomal dysfunction [47], ER stress, nutrient deficiency, mitochondrial damage and pathogen infection [48]. Given that macrolide antibiotics can influence the lysosome, they also potentially activate TFEB and TFE3. Indeed, nuclear translocation of the TFEB-GFP fusion protein was observed in U2OS cells treated with AZD (**Fig. 5A, B**). Likewise, immunofluorescence results showed that the nuclear translocation of TFE3 was also promoted by AZD (**Fig. 5C, D**). Consistently, immunoblot detection of TFEB and TFE3 in the cytoplasm and nucleus showed similar results (**Fig. 5E, F**). Likewise, the activation of TFEB and TFE3 translocation induced by AZD was inhibited by NAC, while the activation of TFEB and TFE3 induced by Torin1 was limited influenced by NAC (**Fig. 5A, C**, Fig. S3A-C). Moreover, AZD induced the lipidation and puncta of LC3B were impeded by the double knockout of TFEB and
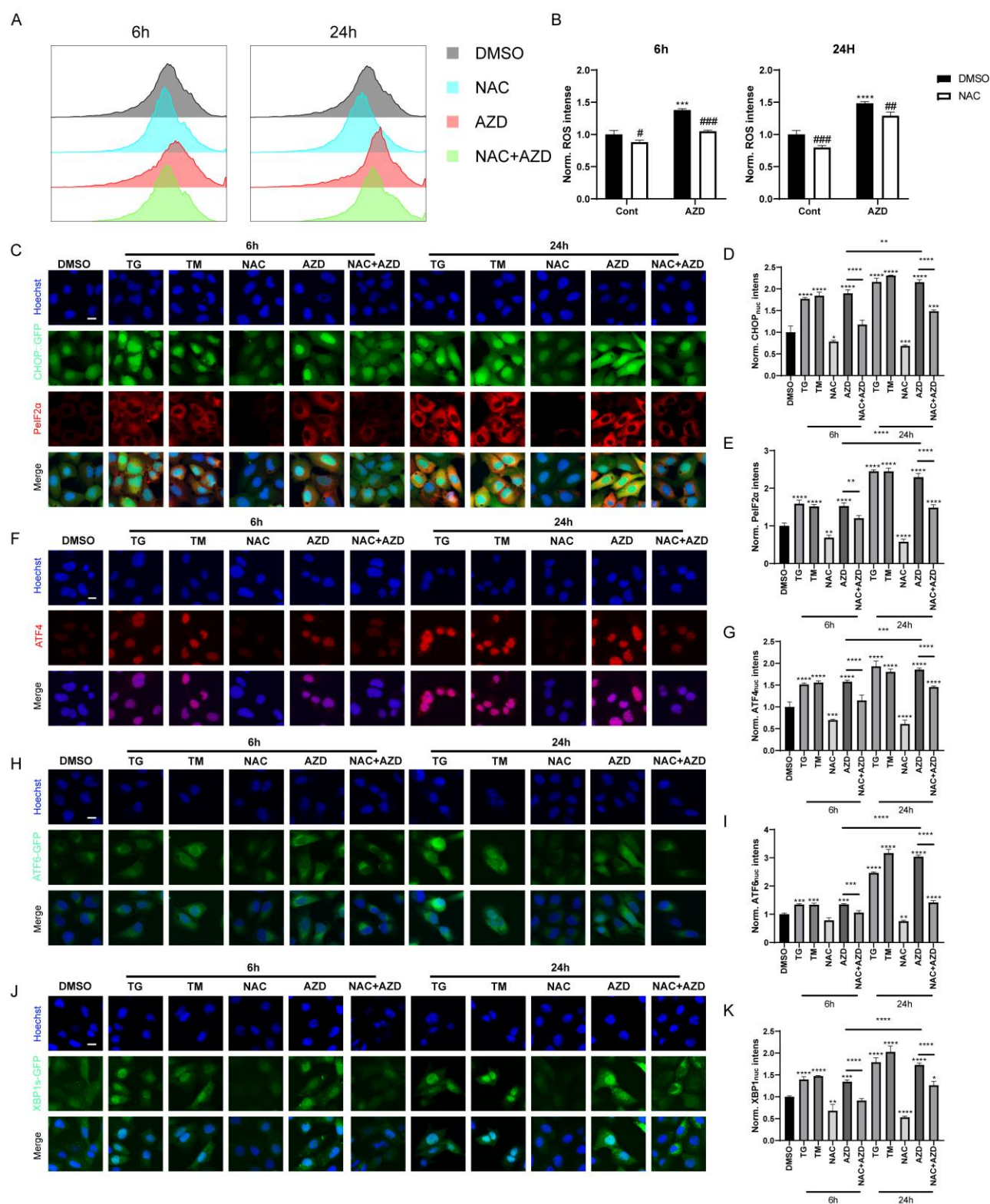
FIGURE 4: AZD induces ROS accumulation and ER stress. (A, B) ROS generation was detected by DCFH-DA probe. MCA205 cells were treated with AZD (40 µM) combined or not with NAC (3 mM) for 6 h or 24 h. Fluorescence intensity histogram **(A)** and average fluorescence intensity **(B)** are presented. **(C-E)** CHOP::GFP-expression U2OS cells were treated with TM (3 µM), TG (3 µM), AZD, NAC or NAC combined AZD for 6 h or 24 h, and PeIF2α was assessed by immunostaining. Representative images are presented **(C)**. The intensity of fluorescence was measured **(D, E)**; **(F-K)** wild type, ATF6-GFP-expression and XBP1s-ΔDBD-venus-expression U2OS cells were treated with TM, TG, AZD, NAC or NAC combined AZD for 6 h or 24 h, then ATF4 was assessed by immunostaining, ATF6 and XBP1s was assessed by GFP intensities. Representative images of ATF4 **(F)**, ATF6 **(H)** and XBP1s **(J)** nuclear translocation are presented. The average nuclear intensity of ATF4 **(G)**, ATF6 **(I)** and XBP1s **(K)** was assessed. Scale bars equal 10 µm. *P<0.05; **P < 0.01; ***P < 0.001; **** P < 0.0001 compared with DMSO. And the horizontal line indicates the comparison between the two groups.
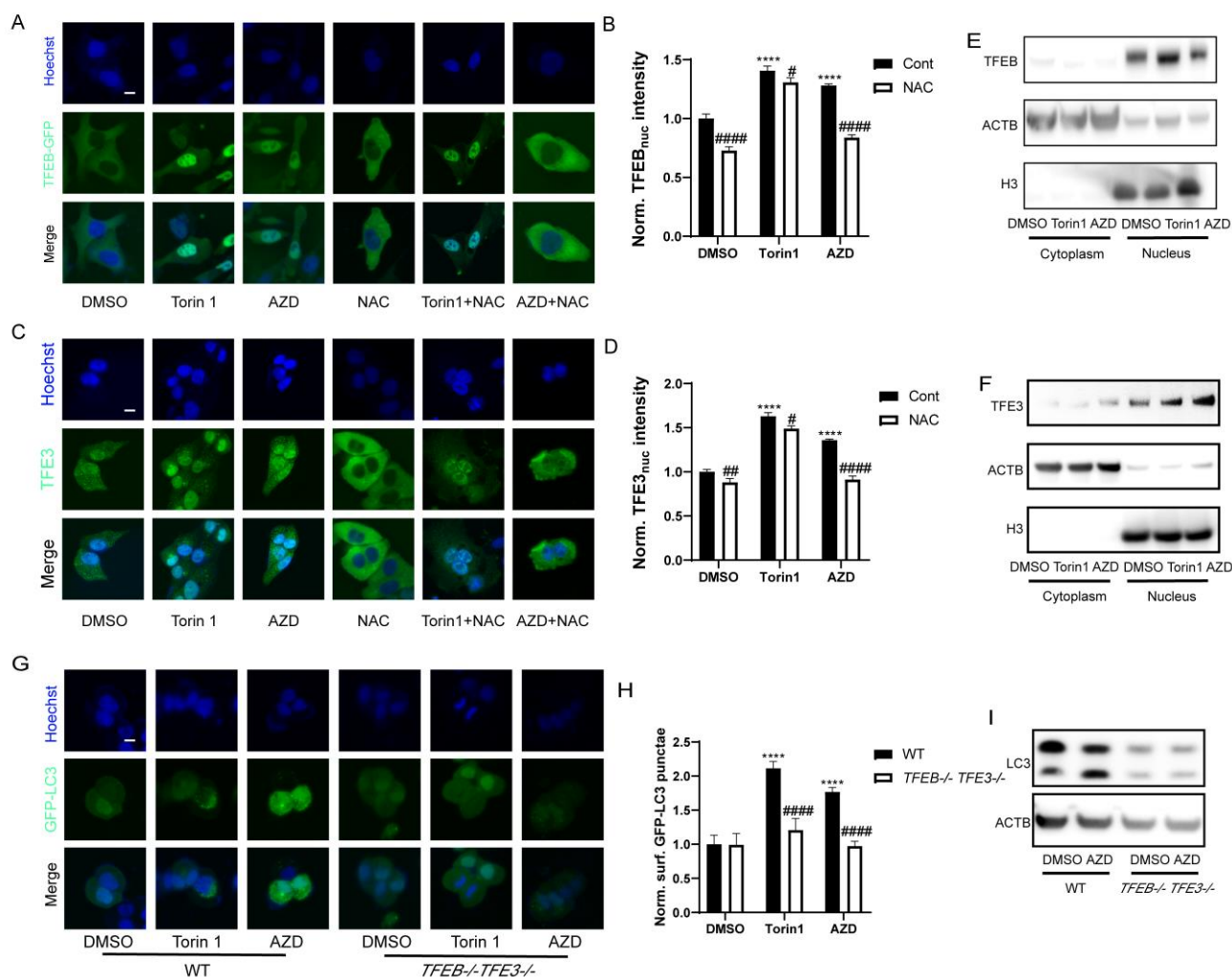
FIGURE 5: AZD induces TFEB/TFE3 activation. (A-F) TFEB-GFP-expressing or wild type U2OS cells were treated with Torin 1 (300 nM) or AZD (40 μM) combined or not with NAC (3 mM) for 6 h. The average nuclear intensity of TFEB was measured **(A, B)**, TFE3 translocation was assessed by immunostaining **(C, D)**, and **(E)** TFEB and **(F)** TFE3 in the cytoplasm and nucleus were assessed by Western blot. **(G)** Western blot was performed for measuring the expression of TFEB and TFE3 in U2OS cells with or without *TFEB-/-TFE3-/-* double-knockout treated with AZD. Scale bars equal 10 μm. (*P < 0.05, **P < 0.01, ***P < 0.001,****P<0.0001 vs. DMSO; #P < 0.05, ##P < 0.01, ###P < 0.001, #### P < 0.0001 vs. Cont or WT).

TFE3 (genotype: *TFEB–/– TFE3–/–*; **Fig. 5G-I**). In addition, interactions between ER stress and TFEB/TFE3 activation induced by AZD were observed. The translocation of TFE3 and accumulation of LC3B induced by AZD were blunted in USOS with a mutant nonphosphorylation of eIF2α (eIF2α$_{S51A}$; Fig. S3D-F). Likewise, *PERK$^{-/-}$* cells exhibited reduced activation of TFE3 (Fig. S4G, H). The activation of CHOP (Fig. S3I, J) and ATF4 (Fig. S3K, L) was inhibited in *TFEB$^{-/-}$ TFE3$^{-/-}$* cells. These results indicate that activation of TFEB and TFE3 represents a key molecular link between ER stress and autophagy induced by AZD.

AZD induced ER stress and promoted tumor growth *in vivo*

Sustained ER stress results in chronic inflammatory responses, which may contribute to cancer genesis and progression [45, 46]. We determined the capacity of AZD to influence tumor growth *in vivo* by measuring the growth of B16F10 melanoma and MCA205 fibrosarcoma in immunocompetent mice treated with AZD, NAC or a combination (**Fig. 6A**, Fig. S4A). The results indicate that AZD accelerated the progression of tumors (**Fig. 6B**, Fig. S4B, C), increased the accumulation of LC3B, and enhanced the expression of PeIF2α *in vivo* (**Fig 6C-E**), and these effects were attenuated by NAC. These findings indicate that AZD induces ER stress and promotes tumor growth *in vivo*.

DISCUSSION

The current study indicated that macrolide antibiotics, such as AZD, RA, and SP, could reduce autophagic flux by inhibiting lysosomal acidification, and induced ROS accumulation and ROS accumulation-dependent ER stress, including the activation of PeIF2α/ATF4/CHOP signaling, the splicing of
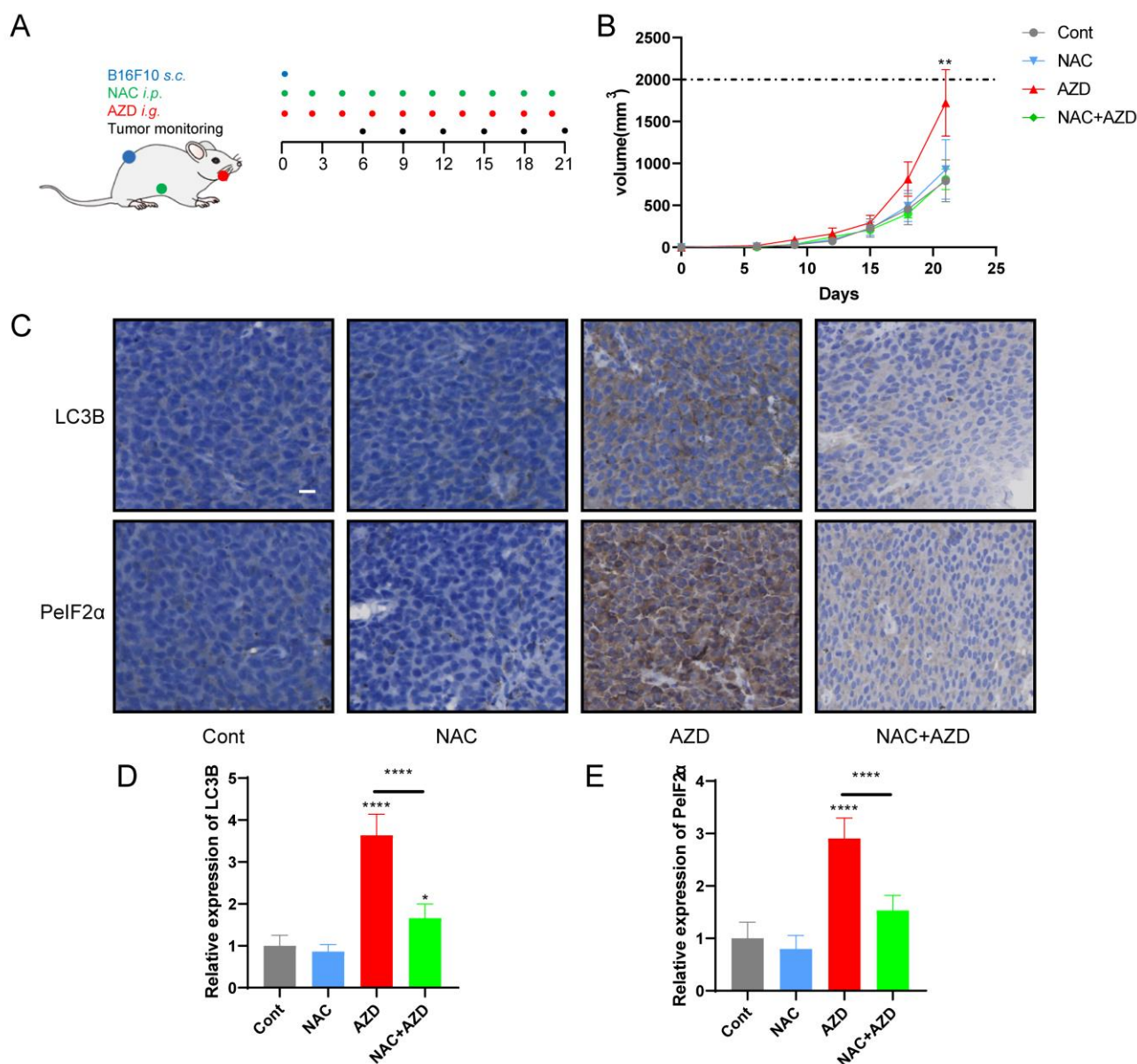
FIGURE 6: NAC reverse AZD-induced tumor growth stimulation. (A-C) *In vivo* treatment of implanted murine B16F10 melanoma with AZD combined or not with NAC (schematic view in A). **(B, C)** The data of administration of AZD combined or not with NAC, depicted as **(C)** growth curves (mean±SD). **(D-F)** Immunohistochemical analysis was performed on paraffin-embedded sections of B16F10 melanoma tissue in mice by using LC3B and eIF2α. Representative images are presented **(D)** and the staining score was assessed **(E, F)**. Scale bars equal 20 µm. *P<0.05; **P < 0.01; ***P < 0.001; **** P < 0.0001 compared with Cont. And the horizontal line indicates the comparison between the two groups.

XBP1, and ATF6 translocation, which contribute to the translocation of TFEB and TFE3. Furthermore, TFEB and TFE3 were involved in the accumulation of LC3B-binding autophagosomes and activation of ATF4 and CHOP (**Fig. 7**). Notably, the use of macrolides has been associated with an increased incidence of malignant tumors, and treatment with AZD promotes tumor growth in a preclinical model in a ROS accumulation and ER stress-dependent manner.

Macrolide antibiotics are a commonly used class of antibiotics composed of a large macrocyclic lactone ring. However, their effect on malignant progression is still ambiguous. On one hand, macrolide drugs have been shown

to retard tumor growth. For example, AZD treatment is reported to reduce tumor cell proliferation in a dose-dependent manner. Mechanistically, AZD could block autophagy-associated degradation to evaluate the levels of death receptors, and then synergize with the effect of tumor necrosis factor-related apoptosis-inducing ligand on apoptosis induction [15]. On the other hand, macrolides combined with β-lactam^{+/−} inhibitors and fluoroquinolones have been found to accelerate tumor growth and to impair the antitumor effects of immune checkpoint inhibitors (ICIs) [6, 52]. Since the antitumor immune response in the host has increasingly exerted a vital effect on malignant
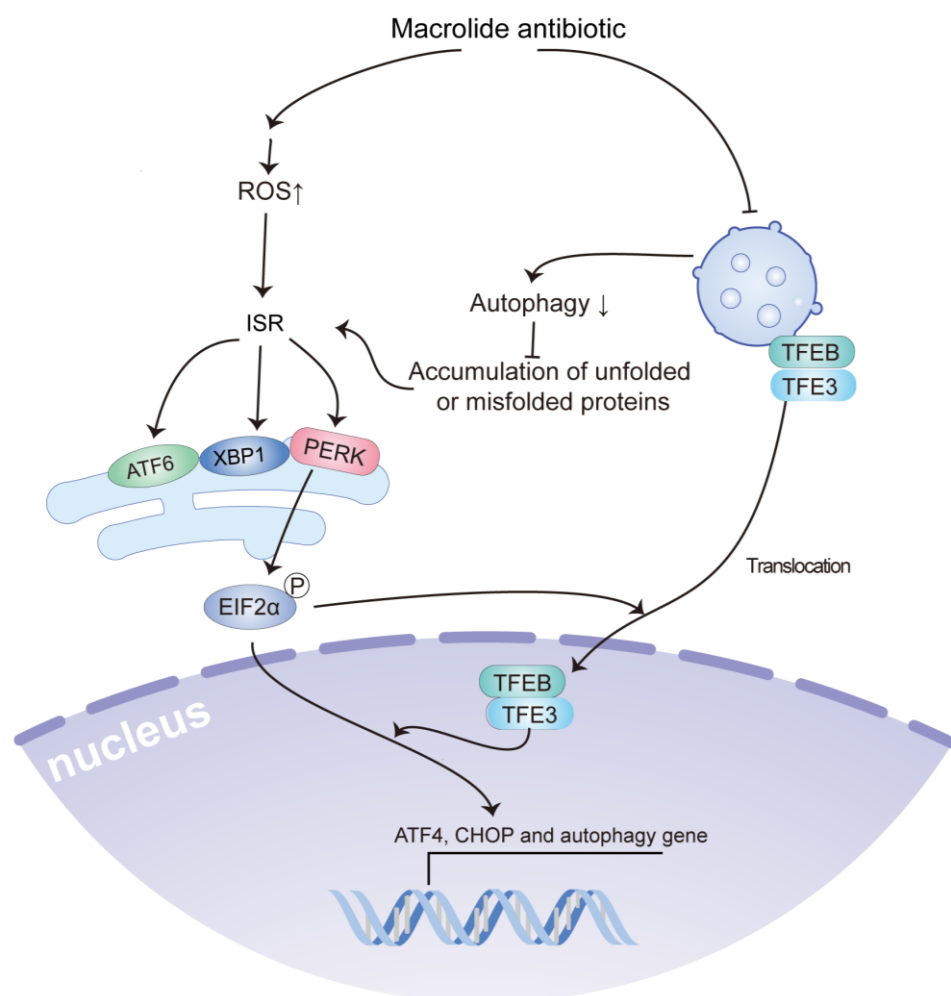
FIGURE 7: Overview of macrolide antibiotics activate the ISR. Macrolide antibiotics inhibit lysosomal acidification, leading to the blockade of autophagic flux and the accumulation of unfolded or misfolded proteins. Moreover, they induce the accumulation of ROS. The combined accumulation of unfolded/misfolded proteins and ROS induces an ISR, including the activation of PeIF2α/ATF4/CHOP signaling, XBP1 splicing, and ATF6 translocation, which in turn contribute to the translocation of TFEB and TFE3. Furthermore, TFEB and TFE3 are involved in the accumulation of LC3B-bound autophagosomes and the activation of ATF4 and CHOP.

disease, the different results may depend on the disparity of mouse models. Furthermore, in an antibiotic-treated group, there was significantly shorter overall survival and progression-free survival [6, 53].

Recent studies have shown that long-term AZD treatment is capable of increasing the levels of ROS and releasing ROS into diverse tissues and organs [57]. At mild concentrations, ROS can stimulate oncogenesis and support tumor proliferation[58]. The evidence suggests that AZD can promote ROS accumulation by inducing mitochondrial dysfunction at doses that do not cause autophagy blockade [44]. Considering that autophagy blockade is also a trigger for ROS accumulation [59], AZD may induce ROS accumulation through multiple pathways. ISR is remarked upon by eIF2α phosphorylation and activation of its downstream pathways is required for initiation of autophagy, UPR, redox homeostasis, and defense against viral infections [22]. Moderate ISR can facilitate tumor growth and metastasis by promoting EMT, tumor cell dormancy, and tumor initiating cell function, as well as supporting tumor immune evasion and angiogenesis [27]. Recent studies have shown that AZD, as autophagy blocker, stimulates ISR in infectious diseases, neurogenic disorders and cancer [29, 54-56].

Likewise, activation of eIF2α and TFEB endows cancer cells with the capacity to increase antioxidant transcription factors and generate antioxidant substances, which assists tumor cells to maintain oxidant-antioxidant homeostasis [28, 60]. Thus, AZD may promote tumorigenesis by inducing a moderate increase in ROS levels. Ultimately, the homeostasis of gut microbiota has emerged as a key factor that impacts tumorigenesis and the tumor-specific immune response [52, 61]. Antibiotic therapy, such as macrolide application, markedly reduces the diversity of gut microbiota, and specifically eliminates some beneficial commensal bacteria, consequently leading to a loss of protective functions for the host. Hence, further fundamental studies and intense clinical trials are required to develop multiple approaches containing selective antibiotic therapy or probiotic transplantation. Currently, AZD is widely considered a safe antibiotic by most practitioners and is commonly used to treat various bacterial infections. Based on the results of this study, the potential risks and benefits for cancer patients should be carefully evaluated to determine whether AZD prescriptions should be issued.

In conclusion, this study provides evidence that macrolide antibiotics may contribute to malignant progression by

inhibiting autophagy, inducing ROS accumulation, and activating ISR. The potential role of macrolide antibiotics in cancer development and progression should be taken into consideration in their clinical use. Further studies are needed to investigate the optimal use of macrolide antibiotics in patients with cancer and to explore the mechanisms underlying their effects on malignant progression.

MATERIALS AND METHODS
Ethics approval and consent to participate
All procedures performed in this study were carried out according to the principles of the Ethics Committee of Renmin Hospital of Wuhan University. The animal experiments were complied with the principles of the Animal Centre of the Renmin Hospital of Wuhan University.

Meta-analysis
Search strategy and source
Relevant studies were searched from the Embase, PubMed and Web of Science databases from January, 2000 to October, 2021. The following terms were used for searching: "antibiotic," "antibacterial agent," "cancer," "neoplasm," "carcinoma" and "risk". The referenced articles of the included publications were also reviewed.

Selection criteria
Two researchers (XY, ZJG) individually performed the search and assessment of all publications acquired.
The inclusion criteria were as follows:
    (a) Case–control or cohort study.
    (b) Original data comparing the risk of primary cancer between ever-users of macrolide antibiotics and nonuser were provided.
    (c) Sufficient data to estimate risk estimates, including hazard ratios (HRs), risk ratios (RRs) and odds ratios (ORs), were available.
The exclusion criteria were as follows:
    (a) *In-vitro* experiment, animal study, reviews, case-reports, cross-sectional studies, letters.
    (b) Irrelevant exposure.
    (c) Duplicate publications (the latest was selected).

Data extraction
The following data was extracted:
    (a) study characteristics, including author, year, country, tumour type, sample size, and study setting and design.
    (b) risk estimates, including HRs, RRs and ORs.

Quality assessment
Two researchers (XY, ZJG) independently conducted the quality assessment of the included studies. The Newcastle–Ottawa scale [62] was utilized to assess the quality of all studies included. A higher score indicated better methodological quality.

Statistical methods
The meta-analysis was conducted using the "meta" package of R software (version 4.0). Pooled risk estimates were calculated and displayed as RRs with corresponding 95% CIs. Heterogeneity among studies was assessed through the I^2 test and Cochrane Q test [63] ($P<0.1$ or $I^2 >50\%$ define substantial heterogeneity). Random-effects model was adapted to create forestplots if heterogeneity was present, otherwise, the fixed-effects model was adapted. Publication bias was evaluated through the Begg's test and Egger's test ($p< 0.05$ define substantial publication bias). Constancy of results was confirmed through sensitivity analysis.

Cell culture and chemicals
GFP-Q74-expressing PC12 (Rat adrenal gland cells) cells were maintained in RPMI-1640 containing 10% horse serum and 5% fetal bovine serum (FBS) [64]. U2OS (human osteosarcoma cells) wild type (wt) and its variants with PERK-deficient (PERK−/−), TFEB and TFE3 double-knockout (*TFEB−/−TFE3−/−*), eIF2α mutant (S51A, non-phosphorylation eIF2α) or stably expressing GFP-LC3B, RFP-LC3B, GFP-ATG4-RFP-LC3BΔG3, mCherry-GFP-p62, GFP::CHOP, ATF6-GFP, TFEB-GFP or XBP1s-ΔDBD-venus and murine melanoma B16F10 cells and murine fibrosarcoma MCA205 cells were cultured in DMEM containing 10% FBS. Cell culture consumables were obtained from Life Technologies (Carlsbad, California, USA), and plastic materials were obtained from Corning (Corning, NY, USA) and Greiner Bio-One (Kremsmünster, Austria). U2OS cell lines with PERK-deficient (*PERK−/−*), TFEB and TFE3 double-knockout (*TFEB−/−TFE3−/−*), eIF2α mutant (S51A, non-phosphorylation eIF2α) and stably expressing GFP-LC3B, RFP-LC3B, GFP-ATG4-RFP-LC3BΔG3, mCherry-GFP-p62, LAMP1-GFP and GFP-LC3, GFP::CHOP, ATF6-GFP, GFP-TFEB or XBP1s-ΔDBD-venus were constructed in the past[29, 42, 65]. Macrolides were obtained from Target Mol (Boston, USA), Torin 1, Baf A1, TG and TM and NAC were from Sigma-Aldrich (Missouri, USA). Cells were treated with macrolides (40 μM), Torin 1 (300 nM), Baf A1 (100 nM), TG (3 μM), TM (3 μM) and NAC (3 mM).

High-content microscopy
Cells were seeded in 384-well black imaging plates at a density of 2000 cells per well and allowed to adapt overnight. Cells were treated with the indicated agents 6 h for detecting the expression of GFP-LC3, RFP-LC3, Q74-GFP and GFP-TFEB, 6 h and 24 h for detecting the expression of CHOP::GFP, GFP-ATF6 and XBP1s-ΔDBD-venus, then fixed with 3.7% paraformaldehyde (Sigma-Aldrich) in PBS at 4°C overnight and then stained with 1 μg/ml Hoechst 33342 (Sigma-Aldrich), and examined using automated microscopy. Each experiment was analyzed at least in triplicate. Image acquisition was performed using an ImageXpress Micro XL automated microscope (Molecular Devices, Sunnyvale, California, USA) equipped with a 20 X Plan-Apo objective (Nikon, Tokyo, Japan). The MetaXpress software (Molecular Devices) was used to define and segment the cellular areas of interest, cytoplasm and nucleus, by excluding cellular debris and dead cells from the dataset. After normalization and statistical evaluation of the parameters of interest, the results are graphically depicted using R software. Finally, images are extracted and pixel intensities are scaled to be visible, ensuring that the same extent is used for all images in a given experiment.

Immunofluorescence
Cells were treated with the indicated agents 6 h for detecting the expression of TFE3, CHOP, 6 h and 24 h for detecting the expression of PeIF2α, 6 h,16 h and 24 h for detecting the expression of ATF4, then fixed with 3.7% paraformaldehyde (Sigma-Aldrich) in PBS at 4°C overnight and stained with 1 μg/ml Hoechst 33342 (Sigma-Aldrich), permeabilized with

0.1% Triton X100(#X100; Sigma-Aldrich), blocked with 5% bovine serum albumin (BSA) in PBS for 1 h, incubated with primary antibody at 4°C overnight, and then incubated with AlexaFluor conjugates 2 h at room temperature (RT; Thermo Fisher Scientific). At last, cells were imaged with automated fluorescence microscopy as described above. The antibodies used are listed in Table S3.

Fluorescent LysoSensor

LysoSensor™ Green DND-189 from ThermoFisher Scientific was used to assess lysosome function in live cells. Cells were washed and stained with 5 µM LysoSensor™ Green DND-189 for 30 min in a 37°C incubator. Then cells were imaged using automated fluorescence microscopy as described above.

Immunoblotting

As described previously [42], cells were washed twice with ice-cold PBS, and then collected with SDS loading buffer. After boiling for 10 min, the proteins were separated by SDS-PAGE, transferred to a nitrocellulose membrane, and detected with specific antibodies at 4 °C overnight, and then incubated with HRP-conjugated secondary antibody (CliniScience) for 2 h at RT. Antibodies are listed in Table S3.

RNA isolation and Real-time PCR

Total RNA was extracted from samples using TRIzol (Pufei, Shanghai) according to the manufacturer's instructions. cDNA was synthesized with the Reverse Transcript Kit (Promega). Real-time PCR was performed with SYBR Green Master Mixture (TAKARA) on the Real-time PCR Detection System (Roche) in triplicate. Glyceraldehyde-3-phosphate dehydrogenase (GAPDH) was used as an endogenous normalization control. Quantification was based on the cycle threshold (Ct) value and calculated by the $2-\Delta\Delta Ct$ method. The sequences of the primers are listed in Table S4.

Determination of ROS generation by flow cytometry

Intracellular ROS was measured by fluorescent dichlorofluorescein converted from cell permeable 2',7'-dichlorofluorescein diacetate (DCFH-DA, Beyotime, Shanghai, China) through oxidative conversion. Cells treated with AZD (40 µM, Sigma-Aldrich) with or without NAC (3 mM) and then incubated with DCFH-DA (10 µM, 20 min, 37°C). Finally, ROS production in cells was measured fluorometrically at wavelengths of 488nm for excitation and 525nm for emission (F-4000, HITACHI, Japan).

Animal experimentation

Seven-week-old female wild-type C57BL/6 mice were maintained in a temperature-controlled and pathogen-free environment with 12-h light/dark cycles, with *ad libitum* access to food and water. Mice were given AZD (50 mg/kg, gavage) with or without NAC (100 mg/kg, intraperitoneal injection) every two days. For the B16F10: mice were injected subcutaneously with B16F10 cells ($1*10^6$). These mice were sacrificed when any one of the tumor sizes reached 2000 mm^3. For the MCA205: mice were injected subcutaneously with MCA205 cells ($6*10^5$). Mice were sacrificed when tumor size reached 2000 mm^3 or when signs of obvious discomfort were observed following the Institutional Animal Care and Use Committee of Renmin Hospital of Wuhan University.

Immunohistochemistry (IHC)

Immunohistochemical staining was performed using an automatic staining machine (Leica Bond3). Following dehydration, antigenic epitopes were retrieved with a 10 mM citrate buffer and microwaving for 10 min. Specimens were then incubated with specific antibodies. Primary antibody staining was detected with peroxidase-conjugated IgG (1:500 diluted P0448, Dako, Glostrup, Denmark). Two independent pathologists evaluated the IHC staining results and scored them according to the percentage and intensity of positive tumor cells. The percentage of positive cells was scored as 0 < 10%, 1 = 10–20%, 2 = 21–50% and 3 > 50%. The staining intensity was evaluated as 0 = no staining, 1 = weak staining, 2 =moderate staining and 3 =strong staining. The final protein staining score was calculated by multiplying the percentage score by the intensity score.

Statistical analysis

The data are reported as means ± SD of triplicate determinations, and experiments were repeated at least three times yielding similar results. Statistical significance between two groups was assessed by Student's t test. And the survival data was assessed by Log-rank test. Statistical analyses were performed with GraphPad Prism 8.0. P values <0.05 denote significance.

CONFLICT OF INTEREST

All the authors agree to the submission and consent for publication this paper. The authors have declared that no competing interest exists.

IN PRESS

Please cite this article as: Xin Yu, Ai-Ling Tian, Ping Wang, Juanjuan Li, Juan Wu, Bei Li, Zhou Liu, Siqing Liu, Zhijie Gao, Si Sun, Shengrong Sun, Yi Tu and Qi Wu (**2023**). Macrolide antibiotics activate the integrated stress response and promote tumor proliferation. **Cell Stress**: *in press*.

REFERENCES

1. Armstrong D, Dregan A, Ashworth M, White P, McGee C, de Lusignan S (**2020**). The association between colorectal cancer and prior antibiotic prescriptions: case control study. **Br J Cancer** 122(6): 912-917. doi: 10.1038/s41416-019-0701-5

2. Simin J, Tamimi RM, Engstrand L, Callens S, Brusselaers N (**2020**). Antibiotic use and the risk of breast cancer: A systematic review and dose-response meta-analysis. **Pharmacol Res** 160: 105072. doi: 10.1016/j.phrs.2020.105072

3. Zhang J, Haines C, Watson AJM, Hart AR, Platt MJ, Pardoll DM, Cosgrove SE, Gebo KA, Sears CL (**2019**). Oral antibiotic use and risk of colorectal cancer in the United Kingdom, 1989-2012: a matched case-control study. **Gut** 68(11): 1971-1978. doi: 10.1136/gutjnl-2019-318593

4. Zhang Q-Y, Yan Z-B, Meng Y-M, Hong X-Y, Shao G, Ma J-J, Cheng X-R, Liu J, Kang J, Fu C-Y (**2021**). Antimicrobial peptides: mechanism of action, activity and clinical potential. **Mil Med Res** 8(1): 48. doi: 10.1186/s40779-021-00343-2

5. Pinato DJ, Howlett S, Ottaviani D, Urus H, Patel A, Mineo T, Brock C, Power D, Hatcher O, Falconer A, Ingle M, Brown A, Gujral D, Partridge S, Sarwar N, Gonzalez M, Bendle M, Lewanski C, Newsom-Davis T, Allara E, Bower M (**2019**). Association of Prior Antibiotic Treatment With Survival and Response to Immune Checkpoint Inhibitor Therapy in Patients With Cancer. **JAMA Oncol** 5(12): 1774-1778. doi: 10.1001/jamaoncol.2019.2785

6. Routy B, Le Chatelier E, Derosa L, Duong CPM, Alou MT, Daillere R, Fluckiger A, Messaoudene M, Rauber C, Roberti MP, Fidelle M, Flament C, Poirier-Colame V, Opolon P, Klein C, Iribarren K, Mondragon L, Jacquelot N, Qu B, Ferrere G, Clemenson C, Mezquita L, Masip JR, Naltet C, Brosseau S, Kaderbhai C, Richard C, Rizvi H, Levenez F, Galleron N, et al. (**2018**). Gut microbiome influences efficacy of PD-1-based immunotherapy against epithelial tumors. **Science** 359(6371): 91-97. doi: 10.1126/science.aan3706

7. Teillant A, Gandra S, Barter D, Morgan DJ, Laxminarayan R (**2015**). Potential burden of antibiotic resistance on surgery and cancer chemotherapy antibiotic prophylaxis in the USA: a literature review and modelling study. **Lancet Infect Dis** 15(12): 1429-1437. doi: 10.1016/s1473-3099(15)00270-4

8. Ford AC, Yuan Y, Moayyedi P (**2020**). Helicobacter pylori eradication therapy to prevent gastric cancer: systematic review and meta-analysis. **Gut** 69(12): 2113-2121. doi: 10.1136/gutjnl-2020-320839.

9. Vázquez-Laslop N, Mankin AS (**2018**). How Macrolide Antibiotics Work. **Trends Biochem Sci** 43(9): 668-684. doi: 10.1016/j.tibs.2018.06.011

10. Qin Y, Ma S (**2020**). Recent Advances in the Development of Macrolide Antibiotics as Antimicrobial Agents. **Mini Rev Med Chem** 20(7): 601-625. doi: 10.2174/1389557520666191223160942

11. Broen JCA, van Laar JM (**2020**). Mycophenolate mofetil, azathioprine and tacrolimus: mechanisms in rheumatology. **Nat Rev Rheumatol** 16(3): 167-178. doi: 10.1038/s41584-020-0374-8

12. Kuypers DRJ (**2020**). Intrapatient Variability of Tacrolimus Exposure in Solid Organ Transplantation: A Novel Marker for Clinical Outcome. **Clin Pharmacol Ther** 107(2): 347-358. doi: 10.1002/cpt.1618

13. Zhou L, Gao W, Wang K, Huang Z, Zhang L, Zhang Z, Zhou J, Nice EC, Huang C (**2019**). Brefeldin A inhibits colorectal cancer growth by triggering Bip/Akt-regulated autophagy. **FASEB J** 33(4): 5520-5534. doi: 10.1096/fj.201801983R

14. Yuan N, Song L, Zhang S, Lin W, Cao Y, Xu F, Fang Y, Wang Z, Zhang H, Li X, Wang Z, Cai J, Wang J, Zhang Y, Mao X, Zhao W, Hu S, Chen S, Wang J (**2015**). Bafilomycin A1 targets both autophagy and apoptosis pathways in pediatric B-cell acute lymphoblastic leukemia. **Haematologica** 100(3): 345-356. doi: 10.3324/haematol.2014.113324

15. Qiao X, Wang X, Shang Y, Li Y, Chen SZ (**2018**). Azithromycin enhances anticancer activity of TRAIL by inhibiting autophagy and up-regulating the protein levels of DR4/5 in colon cancer cells in vitro and in vivo. **Cancer Commun** 38(1): 43. doi: 10.1186/s40880-018-0309-9

16. Moriya S, Che XF, Komatsu S, Abe A, Kawaguchi T, Gotoh A, Inazu M, Tomoda A, Miyazawa K (**2013**). Macrolide antibiotics block autophagy flux and sensitize to bortezomib via endoplasmic reticulum stress-mediated CHOP induction in myeloma cells. **Int J Oncol** 42(5): 1541-1550. doi: 10.3892/ijo.2013.1870

17. Mukai S, Moriya S, Hiramoto M, Kazama H, Kokuba H, Che XF, Yokoyama T, Sakamoto S, Sugawara A, Sunazuka T, Ōmura S, Handa H, Itoi T, Miyazawa K (**2016**). Macrolides sensitize EGFR-TKI-induced non-apoptotic cell death via blocking autophagy flux in pancreatic cancer cell lines. **Int J Oncol** 48(1): 45-54. doi: 10.3892/ijo.2015.3237.

18. Komatsu S, Miyazawa K, Moriya S, Takase A, Naito M, Inazu M, Kohno N, Itoh M, Tomoda A (**2012**). Clarithromycin enhances bortezomib-induced cytotoxicity via endoplasmic reticulum stress-mediated CHOP (GADD153) induction and autophagy in breast cancer cells. **Int J Oncol** 40(4): 1029-1039. doi: 10.3892/ijo.2011.1317

19. Fassl A, Brain C, Abu-Remaileh M, Stukan I, Butter D, Stepien P, Feit AS, Bergholz J, Michowski W, Otto T, Sheng Q, Loo A, Michael W, Tiedt R, DeAngelis C, Schiff R, Jiang B, Jovanovic B, Nowak K, Ericsson M, Cameron M, Gray N, Dillon D, Zhao JJ, Sabatini DM, Jeselsohn R, Brown M, Polyak K, Sicinski P (**2020**). Increased lysosomal biomass is responsible for the resistance of triple-negative breast cancers to CDK4/6 inhibition. **Sci Adv** 6(25): eabb2210. doi: 10.1126/sciadv.abb2210

20. Bergeron A, Chevret S, Granata A, Chevallier P, Vincent L, Huynh A, Tabrizi R, Labussiere-Wallet H, Bernard M, Chantepie S, Bay JO, Thiebaut-Bertrand A, Thepot S, Contentin N, Fornecker LM, Maillard N, Risso K, Berceanu A, Blaise D, Peffault de La Tour R, Chien JW, Coiteux V, Socié G (**2017**). Effect of Azithromycin on Airflow Decline-Free Survival After Allogeneic Hematopoietic Stem Cell Transplant: The ALLOZITHRO Randomized Clinical Trial. **JAMA** 318(6): 557-566. doi: 10.1001/jama.2017.9938

21. Cheng GS, Bondeelle L, Gooley T, He Q, Jamani K, Krakow EF, Flowers MED, de Latour RP, Michonneau D, Socié G, Chien JW, Chevret S, Bergeron A (**2020**). Azithromycin Use and Increased Cancer Risk among Patients with Bronchiolitis Obliterans after Hematopoietic Cell Transplantation. **Biol Blood Marrow Transplant** 26(2): 392-400. doi: 10.1016/j.bbmt.2019.10.025

22. Costa-Mattioli M, Walter P (**2020**). The integrated stress response: From mechanism to disease. **Science** 368(6489): eaat5314. doi: 10.1126/science.aat5314

23. Donnelly N, Gorman AM, Gupta S, Samali A (**2013**). The eIF2α kinases: their structures and functions. **Cell Mol Life Sci** 70(19): 3493-3511. doi: 10.1007/s00018-012-1252-6

24. Schwenzer H, Jühling F, Chu A, Pallett LJ, Baumert TF, Maini M, Fassati A (**2019**). Oxidative Stress Triggers Selective tRNA Retrograde Transport in Human Cells during the Integrated Stress Response. **Cell Rep** 26(12): 3416-3428.e3415. doi: 10.1016/j.celrep.2019.02.077

25. Kroemer G, Mariño G, Levine B (**2010**). Autophagy and the integrated stress response. **Mol Cell** 40(2): 280-293. doi: 10.1016/j.molcel.2010.09.023

26. Anderson NS, Haynes CM (**2020**). Folding the Mitochondrial UPR into the Integrated Stress Response. **Trends Cell Biol** 30(6): 428-439. doi: 10.1016/j.tcb.2020.03.001

27. Cubillos-Ruiz JR, Bettigole SE, Glimcher LH (**2017**). Tumorigenic and Immunosuppressive Effects of Endoplasmic Reticulum Stress in Cancer. **Cell** 168(4): 692-706. doi: 10.1016/j.cell.2016.12.004

28. Martina JA, Diab HI, Brady OA, Puertollano R (**2016**). TFEB and TFE3 are novel components of the integrated stress response. **EMBO J** 35(5): 479-495. doi: 10.15252/embj.201593428

29. Tian A-L, Wu Q, Liu P, Zhao L, Martins I, Kepp O, Leduc M, Kroemer G (**2021**). Lysosomotropic agents including azithromycin, chloroquine and hydroxychloroquine activate the integrated stress response. **Cell Death Dis** 12(1): 6-6. doi: 10.1038/s41419-020-03324-w

30. Pisonero-Vaquero S, Medina DL (**2017**). Lysosomotropic Drugs: Pharmacological Tools to Study Lysosomal Function. **Current Drug Metab** 18(12): 1147-1158. doi: 10.2174/1389200218666170925125940

31. Wang R, Wang J, Hassan A, Lee CH, Xie XS, Li X (**2021**). Molecular basis of V-ATPase inhibition by bafilomycin A1. **Nat Commun** 12(1): 1782. doi: 10.1038/s41467-021-22111-5

32. Velicer CM, Heckbert SR, Lampe JW, Potter JD, Robertson CA, Taplin SH (**2004**). Antibiotic use in relation to the risk of breast cancer. **JAMA** 291(7): 827-835. doi: 10.1001/jama.291.7.827

33. Sørensen HT, Skriver MV, Friis S, McLaughlin JK, Blot WJ, Baron JA (**2005**). Use of antibiotics and risk of breast cancer: a population-based case-control study. **Br J Cancer** 92(3): 594-596. doi: 10.1038/sj.bjc.6602313

34. Kaye JA, Jick H (**2005**). Antibiotics and the risk of breast cancer. **Epidemiology** 16(5): 688-690. doi: 10.1097/01.ede.0000172131.84877.42

35. Tamim HM, Hanley JA, Hajeer AH, Boivin JF, Collet JP (**2008**). Risk of breast cancer in relation to antibiotic use. **Pharmacoepidemiol Drug Saf** 17(2): 144-150. doi: 10.1002/pds.1512

36. Zhang H, García Rodríguez LA, Hernández-Díaz S (**2008**). Antibiotic use and the risk of lung cancer. **Cancer Epidemiol Biomarkers Prev** 17(6): 1308-1315. doi: 10.1158/1055-9965.Epi-07-2817.

37. Tamim HM, Hajeer AH, Boivin JF, Collet JP (**2010**). Association between antibiotic use and risk of prostate cancer. **Int J Cancer** 127(4): 952-960. doi: 10.1002/ijc.25139

38. Tamim HM, Musallam KM, Al Kadri HM, Boivin JF, Collet JP (**2011**). Antibiotic use and risk of gynecological cancer. **Eur J Obstet Gynecol Reprod Biol** 159(2): 388-393. doi: 10.1016/j.ejogrb.2011.06.018

39. Boursi B, Haynes K, Mamtani R, Yang YX (**2015**). Impact of antibiotic exposure on the risk of colorectal cancer. **Pharmacoepidemiol Drug Saf** 24(5): 534-542. doi: 10.1002/pds.3765

40. Boursi B, Mamtani R, Haynes K, Yang YX (**2015**). Recurrent antibiotic exposure may promote cancer formation--Another step in understanding the role of the human microbiota? **Eur J Cancer** 51(17): 2655-2664. doi: 10.1016/j.ejca.2015.08.015

41. Dik VK, van Oijen MG, Smeets HM, Siersema PD (**2016**). Frequent Use of Antibiotics Is Associated with Colorectal Cancer Risk: Results of a Nested Case-Control Study. **Dig Dis Sci** 61(1): 255-264. doi: 10.1007/s10620-015-3828-0

42. Wu Q, Tian AL, Durand S, Aprahamian F, Nirmalathasan N, Xie W, Liu P, Zhao L, Zhang S, Pan H, Carmona-Gutierrez D, Madeo F, Tu Y, Kepp O, Kroemer G (**2020**). Isobacachalcone induces autophagy and improves the outcome of immunogenic chemotherapy. **Cell Death Dis** 11(11): 1015. doi: 10.1038/s41419-020-03226-x

43. Klionsky DJ, Abdel-Aziz AK, Abdelfatah S, Abdellatif M, Abdoli A, Abel S, Abeliovich H, Abildgaard MH, Abudu YP, Acevedo-Arozena A, Adamopoulos IE, Adeli K, Adolph TE, Adornetto A, Aflaki E, Agam G, Agarwal A, Aggarwal BB, Agnello M, Agostinis P, Agrewala JN, Agrotis A, Aguilar PV, Ahmad ST, Ahmed ZM, Ahumada-Castro U, Aits S, Aizawa S, Akkoc Y, Akoumianaki T, et al. (**2021**). Guidelines for the use and interpretation of assays for monitoring autophagy (4th edition)(1). **Autophagy** 17(1): 1-382. doi: 10.1080/15548627.2020.1797280

44. Yu J, Chen X, Zhang Y, Cui X, Zhang Z, Guo W, Wang D, Huang S, Chen Y, Hu Y, Zhao C, Qiu J, Li Y, Meng M, Guo M, Shen F, Zhang M, Zhou B, Gu X, Wang J, Wang X, Ma X, Xu L (**2022**). Antibiotic Azithromycin inhibits brown/beige fat functionality and promotes obesity in human and rodents. **Theranostics** 12(3): 1187-1203. doi: 10.7150/thno.63067

45. Lin Y, Jiang M, Chen W, Zhao T, Wei Y (**2019**). Cancer and ER stress: Mutual crosstalk between autophagy, oxidative stress and inflammatory response. **Biomed Pharmacother** 118: 109249. doi: 10.1016/j.biopha.2019.109249

46. Hasan A, Rizvi SF, Parveen S, Pathak N, Nazir A, Mir SS (**2022**). Crosstalk Between ROS and Autophagy in Tumorigenesis: Understanding the Multifaceted Paradox. **Front Oncol** 12(852424). doi: 10.3389/fonc.2022.852424

47. Zhitomirsky B, Yunaev A, Kreiserman R, Kaplan A, Stark M, Assaraf YG (**2018**). Lysosomotropic drugs activate TFEB via lysosomal membrane fluidization and consequent inhibition of mTORC1 activity. **Cell Death Dis** 9(12): 1191. doi: 10.1038/s41419-018-1227-0

48. Raben N, Puertollano R (**2016**). TFEB and TFE3: Linking Lysosomes to Cellular Adaptation to Stress. **Ann Rev Cell Dev Biol** 32: 255-278. doi: 10.1146/annurev-cellbio-111315-125407

49. Hetz C, Zhang K, Kaufman RJ (**2020**). Mechanisms, regulation and functions of the unfolded protein response. **Nat Rev Mol Cell Biol** 21(8): 421-438. doi: 10.1038/s41580-020-0250-z

50. Smith M, Wilkinson S (**2017**). ER homeostasis and autophagy. **Essays Biochem** 61(6): 625-635. doi: 10.1042/ebc20170092

51. Senft D, Ronai ZA (**2015**). UPR, autophagy, and mitochondria crosstalk underlies the ER stress response. **Trends Biochem Sci** 40(3): 141-148. doi: 10.1016/j.tibs.2015.01.002

52. Derosa L, Routy B, Desilets A, Daillère R, Terrisse S, Kroemer G, Zitvogel L (**2021**). Microbiota-Centered Interventions: The Next Breakthrough in Immuno-Oncology? **Cancer Discov** doi: 10.1158/2159-8290.Cd-21-0236

53. Kilkkinen A, Rissanen H, Klaukka T, Pukkala E, Heliövaara M, Huovinen P, Männistö S, Aromaa A, Knekt P (**2008**). Antibiotic use predicts an increased risk of cancer. **Int J Cancer** 123(9): 2152-2155. doi: 10.1002/ijc.23622

54. Renna M, Schaffner C, Brown K, Shang S, Tamayo MH, Hegyi K, Grimsey NJ, Cusens D, Coulter S, Cooper J, Bowden AR, Newton SM, Kampmann B, Helm J, Jones A, Haworth CS, Basaraba RJ, DeGroote MA, Ordway DJ, Rubinsztein DC, Floto RA (**2011**). Azithromycin blocks autophagy and may predispose cystic fibrosis patients to

mycobacterial infection. **J Clin Invest** 121(9): 3554-3563. doi: 10.1172/jci46095

55. Waetzig V, Riffert J, Cordt J, Reinecke K, Haeusgen W, Boehm R, Cascorbi I, Herdegen T (**2017**). Neurodegenerative effects of azithromycin in differentiated PC12 cells. **E J Pharmacol** 809: 1-12. doi: 10.1016/j.ejphar.2017.05.002

56. Tsubouchi K, Araya J, Minagawa S, Hara H, Ichikawa A, Saito N, Kadota T, Sato N, Yoshida M, Kurita Y, Kobayashi K, Ito S, Fujita Y, Utsumi H, Yanagisawa H, Hashimoto M, Wakui H, Yoshii Y, Ishikawa T, Numata T, Kaneko Y, Asano H, Yamashita M, Odaka M, Morikawa T, Nakayama K, Nakanishi Y, Kuwano K (**2017**). Azithromycin attenuates myofibroblast differentiation and lung fibrosis development through proteasomal degradation of NOX4. **Autophagy** 13(8): 1420-1434. doi: 10.1080/15548627.2017.1328348

57. Parnham MJ, Erakovic Haber V, Giamarellos-Bourboulis EJ, Perletti G, Verleden GM, Vos R (**2014**). Azithromycin: mechanisms of action and their relevance for clinical applications. **Pharmacol Ther** 143(2): 225-245. doi: 10.1016/j.pharmthera.2014.03.003

58. Hayes JD, Dinkova-Kostova AT, Tew KD (**2020**). Oxidative Stress in Cancer. **Cancer Cell** 38(2): 167-197. doi: 10.1016/j.ccell.2020.06.001

59. Zhou J, Li XY, Liu YJ, Feng J, Wu Y, Shen HM, Lu GD (**2022**). Full-coverage regulations of autophagy by ROS: from induction to maturation. **Autophagy** 18(6): 1240-1255. doi: 10.1080/15548627.2021.1984656

60. Bai X, Ni J, Beretov J, Wasinger VC, Wang S, Zhu Y, Graham P, Li Y (**2021**). Activation of the eIF2α/ATF4 axis drives triple-negative breast cancer radioresistance by promoting glutathione biosynthesis. **Redox Biol** 43(101993). doi: 10.1016/j.redox.2021.101993

61. Zhou CB, Zhou YL, Fang JY (**2021**). Gut Microbiota in Cancer Immune Response and Immunotherapy. **Trends Cancer** 7(7):647-660. doi: 10.1016/j.trecan.2021.01.010

62. Wells GA, Shea B, O'Connell J (**2014**). The Newcastle-Ottawa Scale (NOS) for Assessing The Quality of Nonrandomised Studies in Meta-analyses. Available at: https://www.ohri.ca/programs/clinical_epidemiology/oxford.asp. [Accessed 2000]

63. Higgins J, Thompson SG, Decks JJ, Altman DGJBMJ (**2003**). Measuring inconsistency in meta-analyses. BMJ 327(7414): 557-560. doi: 10.1136/bmj.327.7414.557

64. Wang Y, Xie W, Humeau J, Chen G, Liu P, Pol J, Zhang Z, Kepp O, Kroemer G (**2020**). Autophagy induction by thiostrepton improves the efficacy of immunogenic chemotherapy. **J Immunothe Cancer** 8(1). doi: 10.1136/jitc-2019-000462

65. Wu Q, Tian A-L, Li B, Leduc M, Forveille S, Hamley P, Galloway W, Xie W, Liu P, Zhao L, Zhang S, Hui P, Madeo F, Tu Y, Kepp O, Kroemer G (**2021**). IGF1 receptor inhibition amplifies the effects of cancer drugs by autophagy and immune-dependent mechanisms. **J Immunothe Cancer** 9(6): e002722. doi: 10.1136/jitc-2021-002722

IN PRESS